

**SKBF**  
**KBS**

**TEKNISK**  
**RAPPORT**

**81-06**

## **Ion diffusion through highly compacted bentonite**

**Tryggve Eriksen**  
Department of Nuclear Chemistry, Royal Institute of  
Technology, Stockholm

**Arvid Jacobsson**  
**Roland Pusch**  
Division Soil Mechanics, University of Luleå 1981-04-29

**SVENSK KÄRNBRÄNSLEFÖRSÖRJNING AB / PROJEKT KÄRNBRÄNSLESÄKERHET**

*POSTADRESS: Kärnbränslesäkerhet, Box 5864, 102 48 Stockholm, Telefon 08-67 95 40*

ION DIFFUSION THROUGH HIGHLY COMPACTED BENTONITE

Trygve Eriksen

Department Nuclear Chemistry,  
Royal Institute of Technology, Stockholm

Arvid Jacobsson  
Roland Pusch

Division Soil Mechanics, University of Luleå

1981-04-29

This report concerns a study which was conducted for the KBS project. The conclusions and viewpoints presented in the report are those of the author(s) and do not necessarily coincide with those of the client.

A list of other reports published in this series during 1981, is attached at the end of this report. Information on KBS technical reports from 1977-1978 (TR 121), 1979 (TR 79-28) and 1980 (TR 80-26) is available through SKBF/KBS.

## ABSTRACT

Compacted Na- and Ca-bentonites were contacted with aqueous solutions of  $^{134}\text{Cs}^+$ ,  $^{85}\text{Sr}^{2+}$ ,  $^{131}\text{I}^-$  and  $^{36}\text{Cl}^-$  and the diffusivities calculated from tracer concentration - distance profiles in the bentonites 10 days after the onset of diffusion.

In the case of  $^{131}\text{I}^-$  and  $^{36}\text{Cl}^-$  the diffusivities were also determined by measuring the steady state transport through a 5 mm thick bentonite disc.

The experimental results  $D_{\text{Sr}^{2+}}$  (2.3-4.8)  $\times 10^{-11}$ ,  $D_{\text{Cs}^+}$  (0.34-0.75)  $\times 10^{-11}$ ,  $D_{\text{I}^-}$   $1 \times 10^{-12}$  and  $D_{\text{Cl}^-}$   $6 \times 10^{-12}$   $\text{m}^2\text{sec}^{-1}$  indicate that the diffusion through compacted bentonite is governed by complex mechanisms and cannot be accommodated by a simple pore diffusion model. It seems reasonable to assume that non-sorbing ions migrate in the pore water, while cations also move through smectic crystal lattices, preferably through interlamellar spacings according to an ion-exchange-type model. The very low diffusion rate of the investigated anions, as compared with the corresponding rate in bulk water, verifies that the diffusive resistance is very strong for these ions.

ION DIFFUSION THROUGH HIGHLY COMPACTED BENTONITE

KBS PROJ. 15.16, (15.17) and 12.24

By Trygve Eriksen<sup>1)</sup>, Arvid Jacobsson, and  
Roland Pusch

Luleå 1981-04-29

Div Soil Mechanics, University of Luleå (LuH)

1) Dept. Nuclear Chemistry, Royal Institute of  
Technology (KTH), Stockholm

CONTENTS	Page
INTRODUCTION	1
THE CLAY/WATER/ELECTROLYTE SYSTEM	2
Granulometry and mineralogy	2
Water	2
Crystal structure	3
Microstructure, clay/water interaction	3
EXPERIMENTAL	7
Equipment and clay preparation	7
Diffusion experiments	9
TEST RESULTS	12
DISCUSSION	25
CONCLUSIONS	28
REFERENCES	28

## INTRODUCTION

The KBS concept concerning the storage of unprocessed nuclear fuel wastes implies that the canisters be deposited in drilled holes and isolated from the rock by a clay barrier consisting of highly compacted bentonite. The clay will be applied in the form of precompacted blocks which are shaped so as to fill practically all the space between the canisters and the rock. Since the bentonite is not fully water saturated at its deposition it takes up additional water from the rock, swells and becomes saturated, by which a perfect contact is created between the clay and canister, and between the clay and rock, respectively. The water uptake involves water molecule migration processes of the diffusion type, which makes it possible to predict its rate and distribution (PUSCH, 1980a).

When saturation has taken place and when the temperature, which will be temporarily raised to 60-80 °C in the immediate vicinity of the canisters, has finally dropped to its original level, water flow through the bentonite will be caused only by regional hydraulic gradients. These will be very low and considering the insignificant permeability -  $k < 10^{-13}$  m/s at the expected final bulk density 2.1 t/m<sup>3</sup> - it is concluded that migration of ions leading to canister corrosion as well as to the transfer of radionuclides through the clay when such corrosion has taken place, is governed by diffusion mechanisms and not by flow (PUSCH, 1980 b). This was understood at an early stage of the KBS project and a number of diffusion tests have been conducted to provide data for the determination of ion migration rates (cf. NERETNIEKS, 1978). The present report deals with diffusion experiments in which the influence of microstructural homogeneity and confining filters are especially considered. Also, the distribution coefficient for a linear sorption isotherm  $K_d$  is discussed, the ions studied being Sr<sup>2+</sup>, Cs<sup>+</sup>, Cl<sup>-</sup> and I<sup>-</sup>.

## THE CLAY/WATER/ELECTROLYTE SYSTEM

### Granulometry and mineralogy

Two commercially available bentonites were used for the production of highly compacted clay; the American Colloid Co. type MX-80 (Na-bentonite) being the main KBS reference material, and the Bavarian Erbslöh Ca-bentonite, representing a natural deposit in West Germany.

Both bentonites are characterized by a minus 2  $\mu\text{m}$  content of approximately 85%, and a montmorillonite content of about 80-90% of this fraction. The remaining fraction is mainly silt with quartz and feldspars as dominating minerals, and with micas, sulphides and oxides as accessory constituents. The industrial processing of the clays involves drying and grinding, which yields granulation with aggregate sizes mainly ranging between those of fine silt and fine sand.

The two bentonites are not purely sodium - or calcium - saturated clay materials. Thus, spectrometric analyses have shown that the pore water of the MX-80 material contains 30 mg Ca, 15 mg Mg, and 70 mg Na per liter pore water, while the Erbslöh material contains 20-60 mg Ca, 15-30 mg Mg, and 20-40 mg Na per liter pore water.

### Water

The water saturation of the bentonite samples to yield a practically complete water filling of initially air-containing voids was made by means of the KBS reference water, "Allard's" solution (cf. KBS Report 98) which is a synthetic ground water (91 mg of cations and 215 mg of anions per liter). It is considered to be representative of the ground water at 500 m depth in Swedish crystalline rock.

### Crystal structure

Two possible crystal lattice structures of smectites are known (cf. Fig. 1). Both can be described as a condensation of a silica/oxygen layer on each side of a gibbsite or brucite sheet. Some silicons in tetrahedral coordination are replaced by  $\text{Al}^{3+}$  and/or  $\text{Mg}^{2+}$  while some Al and Mg in octahedral positions are usually replaced by  $\text{Fe}^{3+}$  or  $\text{Li}^+$ , giving rise to lattice charge defects which are (partially) compensated by exchangeable cations. The Hofmann, Endell & Wilm structure ("cis-coordination") is commonly used in literature but there are indications that the Edelman-Favejee type ("trans-coordination"), with a fraction of the silica tetrahedrons being converted, is valid at low and moderate temperatures ( $<100^{\circ}\text{C}$ ). The hydrophilic properties of montmorillonite may thus be associated with the presence of protruding OH-groups (cf. JACOBSSON, 1974).

### Microstructure, clay/water interaction

Neither the rate of water uptake and permeation nor the migration of cations and anions can be understood and properly described without considering the microstructural features of the highly compacted bentonite. They have been touched upon in previous reports (PUSCH, 1980b) but require additional treatment with special reference to interlamellar space and chemical environment.

The microstructure of freshly compacted granulated, "air-dry" bentonite powders is illustrated by Fig. 2.



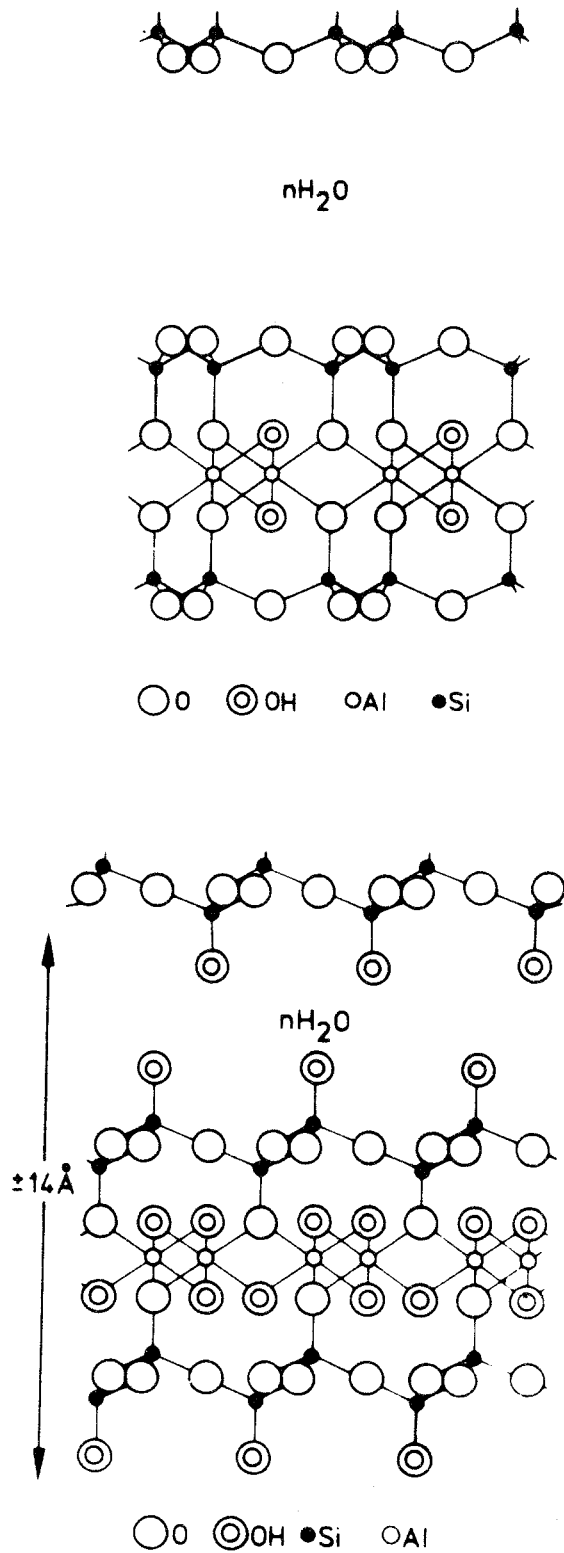


Fig. 1 The crystal structure of montmorillonite. Upper picture shows the model of Hofmann, Endell & Wilm (1933). Lower picture according to Edelman & Favajee.

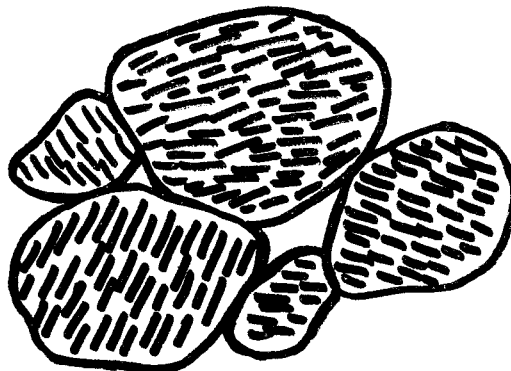


Fig. 2. Schematic picture of the microstructure of freshly compacted MX-80.

The aggregates are characterized by a very small interparticle and interlamellar spacing in the "air-dry" condition. When the bentonite powder is compacted the aggregates are forced together. At moderate pressures and uniaxial compaction as well as at isotropic compaction under any pressure, the overall particle orientation is largely random. Even very high pressures cannot expell all water and produce homogeneous structural patterns so the application of common pressures - 50 to 100 MPa - yields a practically isotropic microstructure characterized by dense aggregates separated by voids. The overall orientation of the montmorillonite particles is largely random.

In the course of water saturation the aggregates expand and, if given sufficient time, most of the larger interparticle voids will be filled by a clay gel formed by the expanding aggregates. Eventually, a condition of

considerable isotropy and homogeneity with respect to particle orientation and interparticle distance will be reached at moderate and high densities ( $>1.5 \text{ t/m}^3$ ).

The average particle spacing, without reference to inter- or intraparticle (interlamellar) distances, is schematically illustrated by Fig. 3.

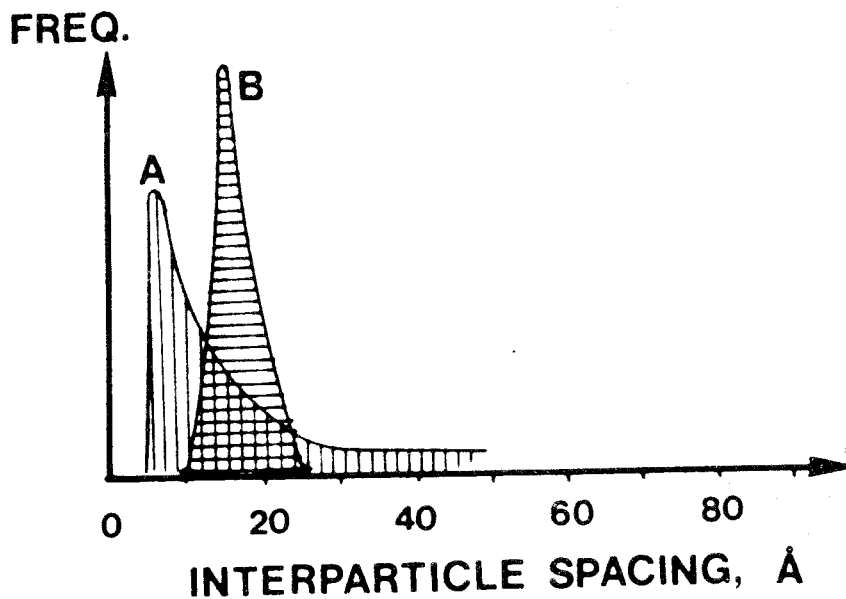


Fig. 3. Schematic distributions of the interparticle (or rather interlamellar) spacing. A) original spectrum for "air-dry" bentonite. B) narrow peak for homogeneous, swollen sample with high density.

The larger swelling ability of Na-bentonite than of Ca versions, which has been documented through a number of tests, suggests that many voids in the latter clay type will not be completely gel-filled when the aggregates expand in course of the saturation. A higher permeability of Ca-bentonite is therefore expected and this has been confirmed experimentally.

## EXPERIMENTAL

### Equipment and clay preparation

The experiments referred to in this report were performed by use of the LuH swelling oedometer (Fig. 4). Each test involved compaction of "air-dry" bentonite to the desired density, and subsequent water uptake under confined conditions which yielded a bulk density of  $2.1 \text{ t/m}^3$  after water saturation of all samples. At the end of the period of water uptake, which led to a degree of water saturation better than 97% and the duration of which was related to the height of the sample, the lower filter was connected to a vessel for the collection of leachate. The upper filter was connected to a cylindrical PVC plastic vessel containing the respective solution. All tests were made at  $25^\circ\text{C}$  or  $70^\circ\text{C}$  with sample heights equal to 0.5 cm or 2.0 cm, meaning that water saturation was obtained after a few days. The development of homogeneous microstructural conditions is expected to require several weeks so all the samples were left to rest for about 6 weeks before the diffusion tests started.

The stainless, non-corrosive steel filters had a void size smaller than  $2.5 \mu\text{m}$ , which is sufficiently small to prevent any but insignificant entering of clay particles into the filters.

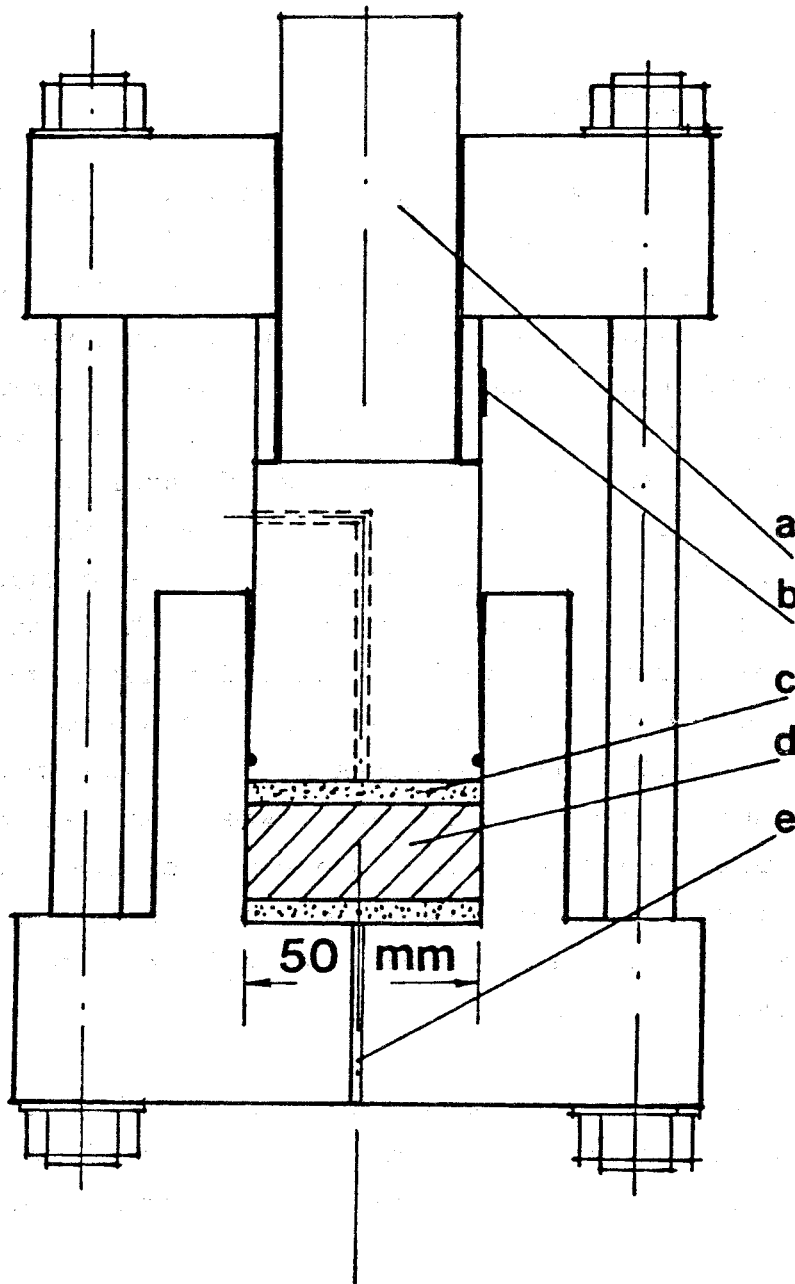


Fig. 4. The LuH swelling pressure oedometer. The compacted sample (d) was confined between the filter stones (c) through which water passed during the period of saturation as well as in the diffusion tests. The "loading piston" (a) was used only to determine, separately, the swelling pressure.

### Diffusion experiments

At the start of each test the water in the upper vessel was replaced by Allard water solution doped with the radionuclides used as tracers. Continuous circulation was applied to yield uniform concentration in the upper as well as the lower vessel.  $^{85}\text{Sr}$ ,  $^{134}\text{Cs}$  and  $^{131}\text{I}$  were selected as tracers because they are  $\gamma$ -emitters and can be easily analyzed without the need of chemical separation.  $\text{Cl}^-$ -diffusion is of great practical importance also, but since chlorine does not have any suitable  $\gamma$ -emitting nuclide the  $\beta$ -emitting  $^{36}\text{Cl}$  was used.

The radionuclides were obtained in aqueous stock solutions as follows:  $^{85}\text{Sr}$  in 0.5 M HCl,  $^{134}\text{Cs}$  as CsCl,  $^{131}\text{I}$  in NaOH (pH7-10) and  $^{36}\text{Cl}$  as NaCl.

Tracer solutions were prepared by diluting small aliquots ( $\mu\text{l}$ ) of the stock solution with Allard water.

Pilot tests were first conducted with 24 ml tracer solutions containing 0.2 MBq and 0.15 MBq of  $^{85}\text{Sr}$  and  $^{134}\text{Cs}$ , respectively. After about 30 days the oedometers were opened and the 20 mm long cylindrical bentonite specimens sliced into 0.5-1 mm thick discs. These were weighed and their radionuclide concentration measured by  $\gamma$ -counting in a 3"x3" NaI well type scintillation detector connected to a 256 channel pulse height analyzer. Counting data were corrected for background radiation and in the case of  $^{85}\text{Sr}$  also for the interference of  $^{134}\text{Cs}$ -decay. After  $\gamma$ -counting the samples were dried and the water content determined. The pilot tests showed that the tracer concentrations in the supply vessel decreased very rapidly and the radionuclides were found to have migrated further into the bentonite than expected. The experimental conditions were therefore modified. The volume of the tracer solutions was increased to 150 ml and  $^{85}\text{Sr}$  and  $^{134}\text{Cs}$

titrated separately into the solution during the experiments to maintain constant tracer concentrations throughout the tests ( $\pm 10\%$ ). Such addition of tracers was not required in the experiments with  $^{131}\text{I}$  and  $^{36}\text{Cl}$ .

In the main test series the oedometers were opened 10 days after the onset of diffusion and the concentration of  $^{85}\text{Sr}$ ,  $^{134}\text{Cs}$  and  $^{131}\text{I}$  measured as described previously. The determination of the concentration of  $^{36}\text{Cl}$  was made in a different way. Each specimen was dispersed in 30 ml distilled water and  $\text{HNO}_3$  then added to the slurry to induce sedimentation of the minerals. After centrifugation, the  $^{36}\text{Cl}$  in the aqueous phase was precipitated as  $\text{AgCl}$  and the  $^{36}\text{Cl}$  concentration of the dried precipitate determined by  $\beta$ -counting with a GM-detector. The evaluation of the total amount of  $^{36}\text{Cl}$  in each bentonite specimen was based on the assumption that the  $^{36}\text{Cl}$  concentration was the same in the aqueous phase as in the pore water of the bentonite after centrifugation i.e. assuming no sorption of  $^{36}\text{Cl}$  on the bentonite.

In the case of  $\text{Cl}^-$  and  $\text{I}^-$  the diffusivities were also determined by measuring the steady-state transport of  $^{36}\text{Cl}$  and  $^{131}\text{I}$  through a 5 mm thick bentonite disc. In these experiments, "break-through" curves were plotted on the basis of  $\beta$ - and  $\gamma$ -counting of 0.5 ml samples from the lower vessel.

The test program is specified in Table 1.

Table 1. Test data.

Test No	Test type	Clay	Ion	Sample height cm	Temp. °C	Remark
1	Concentr.profile	Mx-80	<sup>85</sup> Sr	2	25	Pilot test
2	"-	MX-80	<sup>85</sup> Sr	2	70	"-
3	"-	MX-80	<sup>134</sup> Cs	2	25	"-
4	"-	MX-80	<sup>134</sup> Cs	2	70	"-
5	"-	Erbslöh	<sup>85</sup> Sr	2	25	"-
6	"-	Erbslöh	<sup>85</sup> Sr	2	70	"-
7	"-	Erbslöh	<sup>134</sup> Cs	2	25	"-
8	"-	Erbslöh	<sup>134</sup> Cs	2	70	"-
9	"-	MX-80	<sup>85</sup> Sr	2	25	Main test
10	"-	MX-80	<sup>85</sup> Sr	2	70	"-
11	"-	MX-80	<sup>134</sup> Cs	2	25	"-
12	"-	MX-80	<sup>134</sup> Cs	2	70	"-
13	"-	Erbslöh	<sup>85</sup> Sr	2	25	"-
14	"-	Erbslöh	<sup>85</sup> Sr	2	70	"-
15	"-	Erbslöh	<sup>134</sup> Cs	2	25	"-
16	"-	Erbslöh	<sup>134</sup> Cs	2	70	"-
17	"-	MX-80	<sup>131</sup> I	2	25	"-
18	"-	MX-80	<sup>36</sup> Cl	2	25	"-
19	"-	Erbslöh	<sup>131</sup> Cl	2	25	"-
20	Break-through	MX-80	<sup>131</sup> I	0.5	25	
21	"-	MX-80	<sup>36</sup> Cl	0.5	25	
22	"-	Erbslöh	<sup>131</sup> I	0.5	25	



## TEST RESULTS

### General

The test conditions are of extreme importance in all kinds of experiments which involve transient processes. Thus, curve fitting to determine relevant parameters of applied diffusion equations requires that the tested specimen is homogeneous or that variations in its composition can be expressed in a mathematical form. In the present case of testing the rather long period of rest after water saturation probably led to a fairly high degree of homogeneity in the central parts of the specimens. Close to the filters the conditions are expected to be somewhat different due to the tendency of minute crystallites to migrate into the filter voids and to the difficulty of separating the filters from the adhering clay without changing the water content and density of the clay adjacent to the filter. An important part of the testing was therefore to determine the water content.

### Water content and homogeneity of sectioned samples

All the samples were found to be somewhat wetter at the end which was in contact with the tracer solution. Typical examples are shown in Fig. 5 which also illustrates that the variation in water content is very small in the larger part of the samples. The "excess" water probably originates from the separation of the filter and clay. Water seems to have flown from the filter voids or simply sucked from the filter at the removal of the clay. The resulting moisture anomaly turns out to be of importance in the evaluation of the diffusion coefficients as will be shown in the subsequent text.

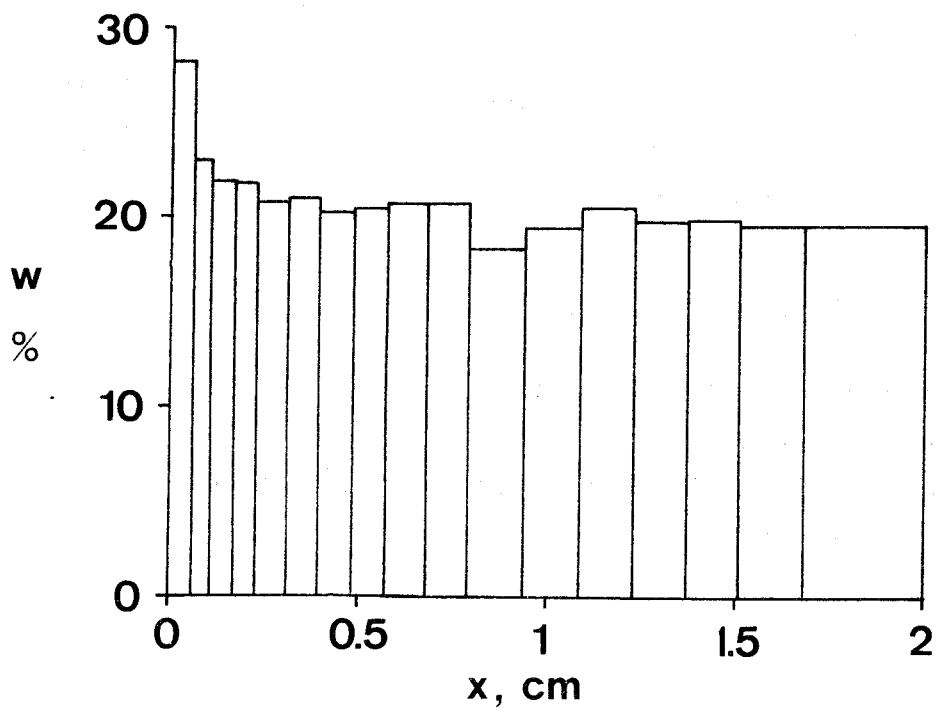
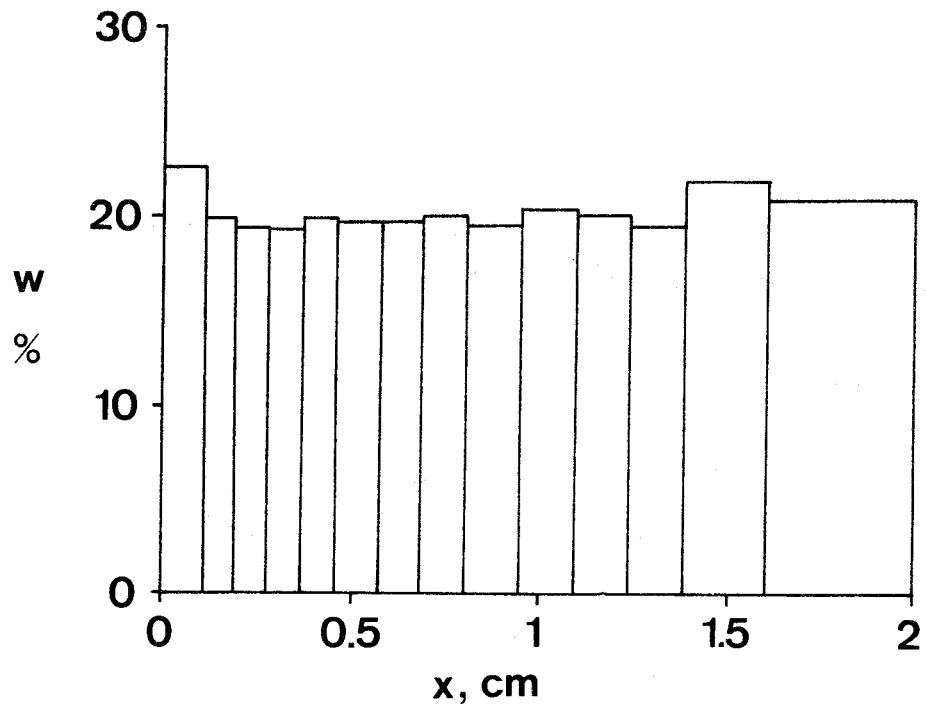


Fig. 5. Variations in water content with distance  $x$  from the interface between filter and clay specimen.

## Evaluation of diffusion coefficients

### Concentration profile analysis

The diffusion coefficients  $D_{obs}$  were evaluated by fitting the experimental data with the equation:

$$c/c_o = \operatorname{erfc} \frac{x}{2\sqrt{D \cdot t}} \quad (1)$$

where  $c$  = tracer concentration at distance  $x$  from the interface between tracer solution and clay

$c_o$  = tracer concentration at the interface between tracer solution and clay

$t$  = time after onset of diffusion

### Break-through tests

For the break-through tests there are only two experimental data to be inserted to satisfy the diffusion equation;  $c_L$  being the activity at the break-through end ("low activity") and  $c_o$  the activity at the interface between tracer solution and clay.  $D_{obs}$  is evaluated by applying the equation:

$$V_L \cdot dc_L/dt = D_{obs} \cdot A \cdot \frac{c_o - c_L}{x} \quad (2)$$

where  $V_L$  = volume of the low activity solution

$A$  = cross section area of bentonite sample

$x$  = distance from the interface between tracer solution and clay

Diffusion of Sr<sup>2+</sup> and Cs<sup>+</sup>

Fig. 6 illustrates a typical distribution pattern of <sup>85</sup>Sr after 13 days of diffusion into a 20 mm long bentonite sample. At the interface between the tracer solution in the upper vessel and the clay, the theoretically expected <sup>85</sup>Sr concentration should be  $K_d \cdot c_s$  where  $K_d$  is the distribution coefficient and  $c_s$  the concentration of the tracer solution. In practice, however, the concentration always turned out to be lower; as an average it was approximately 1/10 of the expected value.

The evaluated diffusion coefficients are given in Table 2. Fig. 7 illustrates typical concentration profiles fitted to experimental data.

Table 2.  $D_{obs}$  for Sr<sup>2+</sup> and Cs<sup>+</sup> diffusion as interpreted from concentration profile analyses of 20 mm long samples.

Bentonite	Temp °C	Ion	$D_{obs}, m^2 \cdot s^{-1}$	
			Pilot tests	Main tests
MX-80	25	Sr <sup>2+</sup>	$2.7 \cdot 10^{-11}$	$2.3 \cdot 10^{-11}$
		Cs <sup>+</sup>	$8.6 \cdot 10^{-12}$	$7.5 \cdot 10^{-12}$
	70	Sr <sup>2+</sup>	$3.1 \cdot 10^{-11}$	$4.1 \cdot 10^{-11}$
		Cs <sup>+</sup>	$2.4 \cdot 10^{-11}$	$4.0 \cdot 10^{-11}$
Erbslöh	25	Sr <sup>2+</sup>	$1.7 \cdot 10^{-11}$	$4.8 \cdot 10^{-11}$
		Cs <sup>+</sup>	$2 \cdot 10^{-13}$	$3.4 \cdot 10^{-12}$
	70	Sr <sup>2+</sup>	$1.1 \cdot 10^{-10}$	$2.6 \cdot 10^{-11}$
		Cs <sup>+</sup>	$1.6 \cdot 10^{-12}$	$4.0 \cdot 10^{-12}$

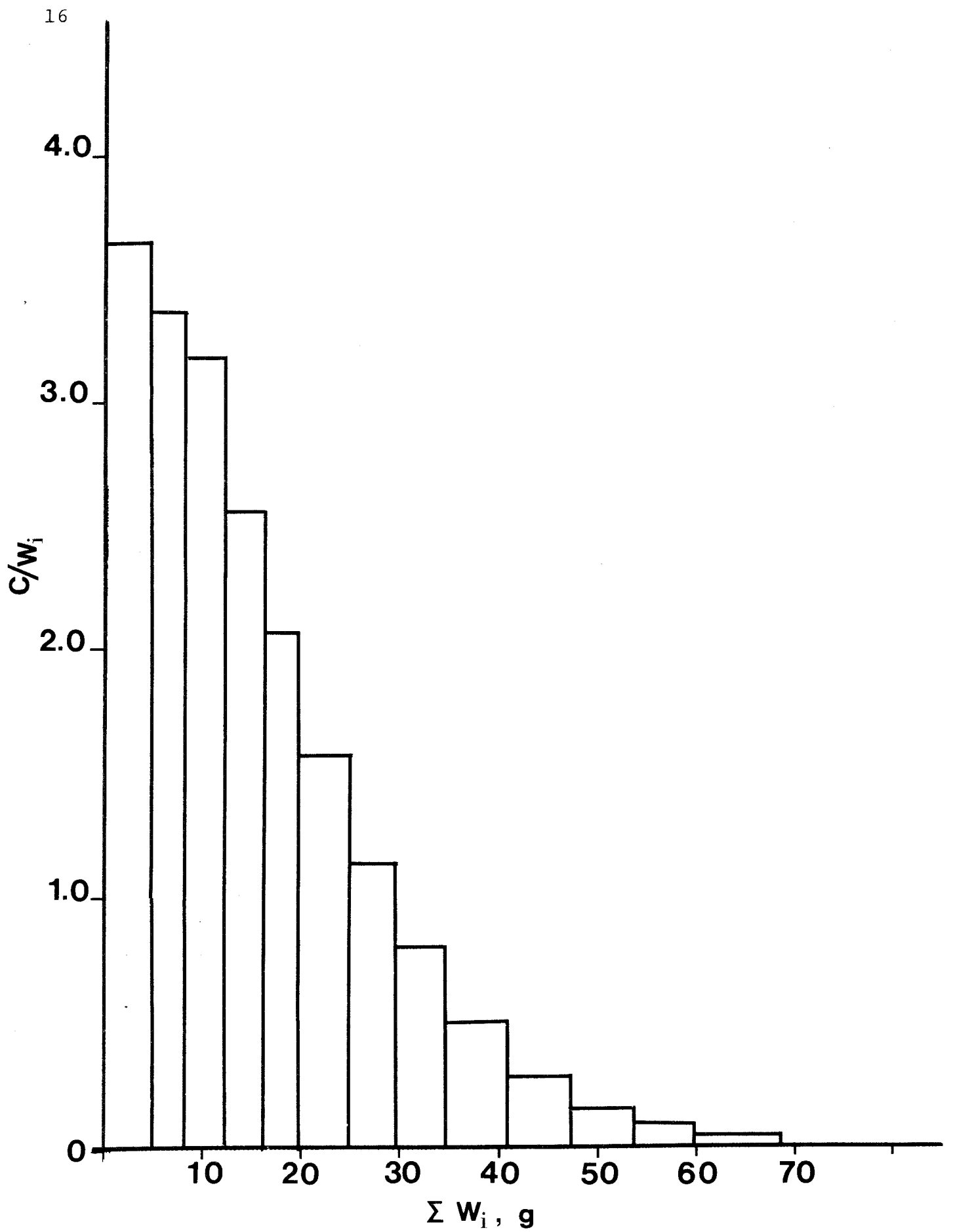


Fig. 6. Concentration profile of  $^{85}\text{Sr}$  in Na-bentonite at  $25^\circ\text{C}$  after 13 days.  $c$  = counts (relative scale) and  $w_i$  = weight of sample.

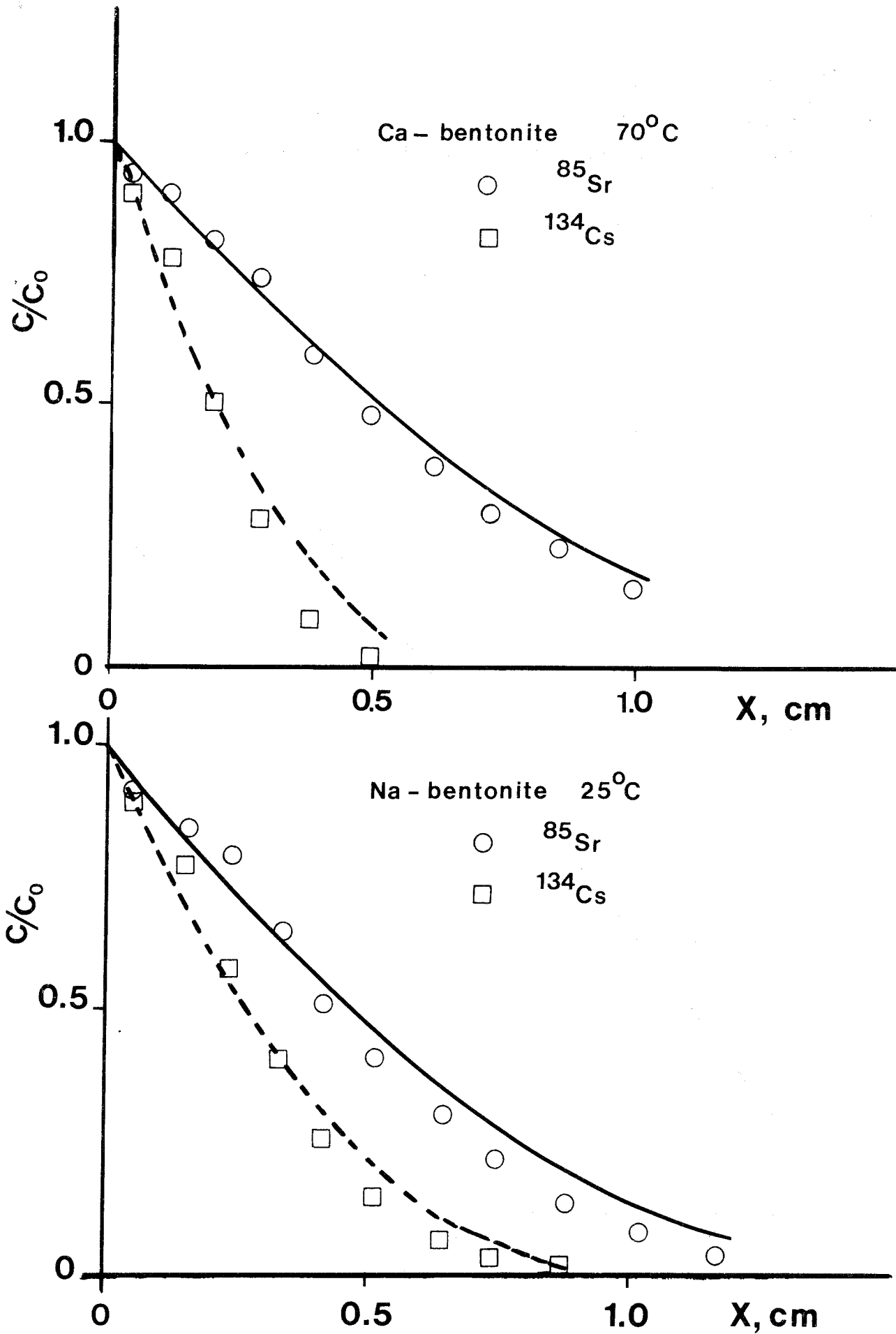


Fig. 7. Concentration profiles calculated from Eq. (1).

Diffusion of  $\text{Cl}^-$  and  $\text{I}^-$ 

Break-through graphs of the diffusive transport of  $\text{I}^-$  and  $\text{Cl}^-$  through 0.5 cm thick MX-80 discs are shown in Figs. 8 and 9, while radionuclide profiles of the same discs are illustrated by Figs. 10 and 11.

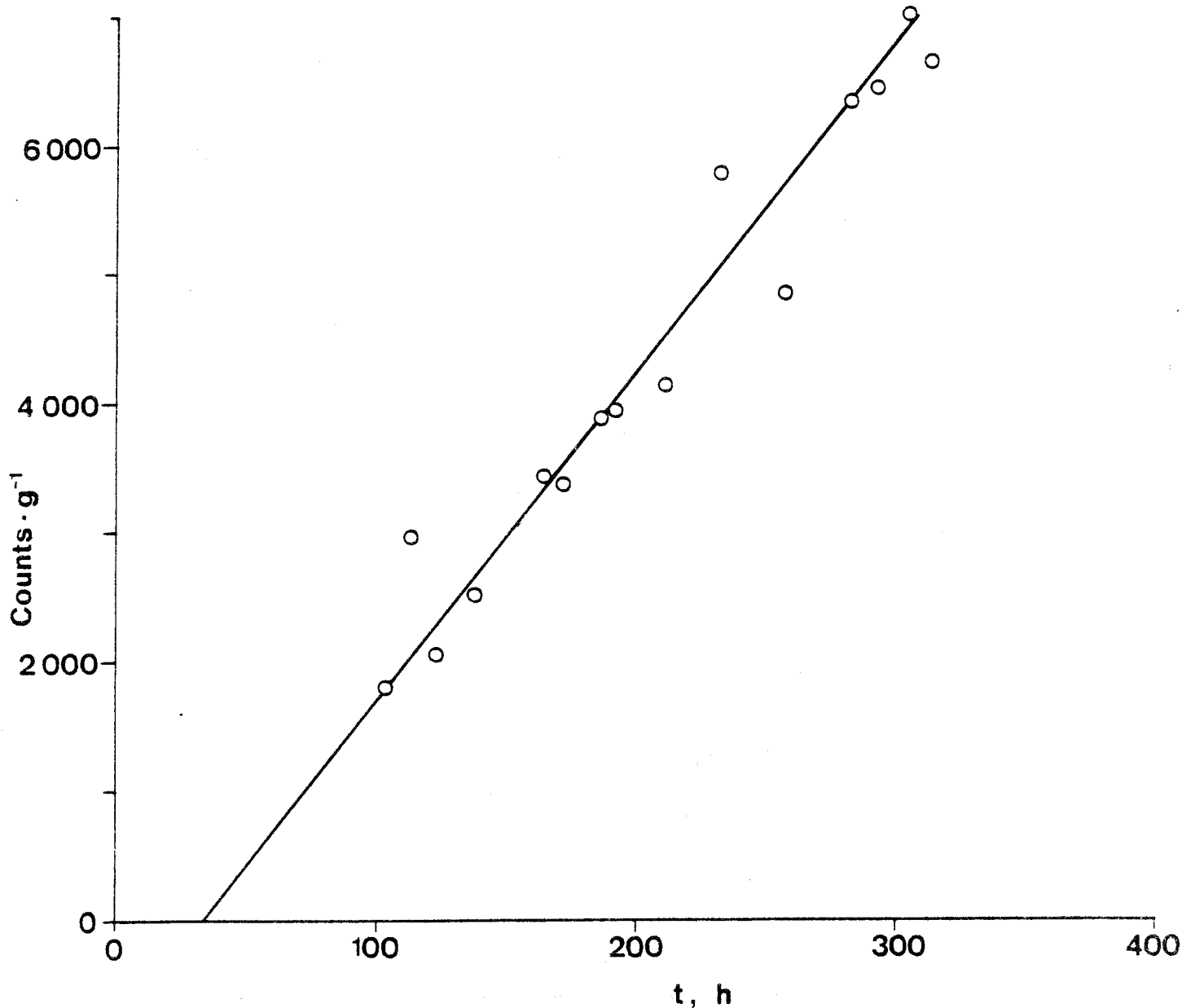


Fig. 8. Diagram of "break-through" of  $\text{I}^-$  indicating a linear relationship between time of diffusion and activation of percolated water mass.

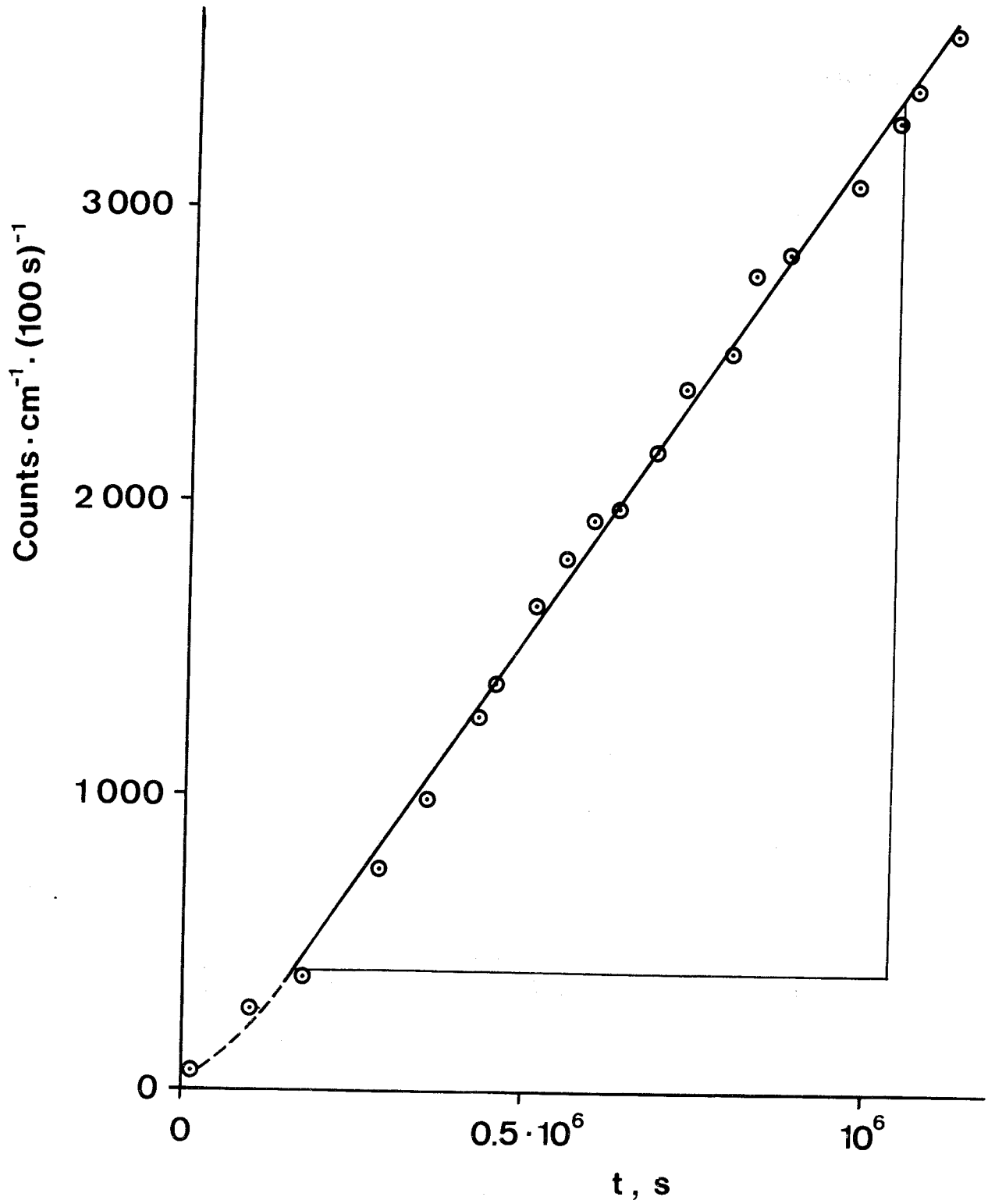


Fig. 9. Diagram of break-through test of Cl .



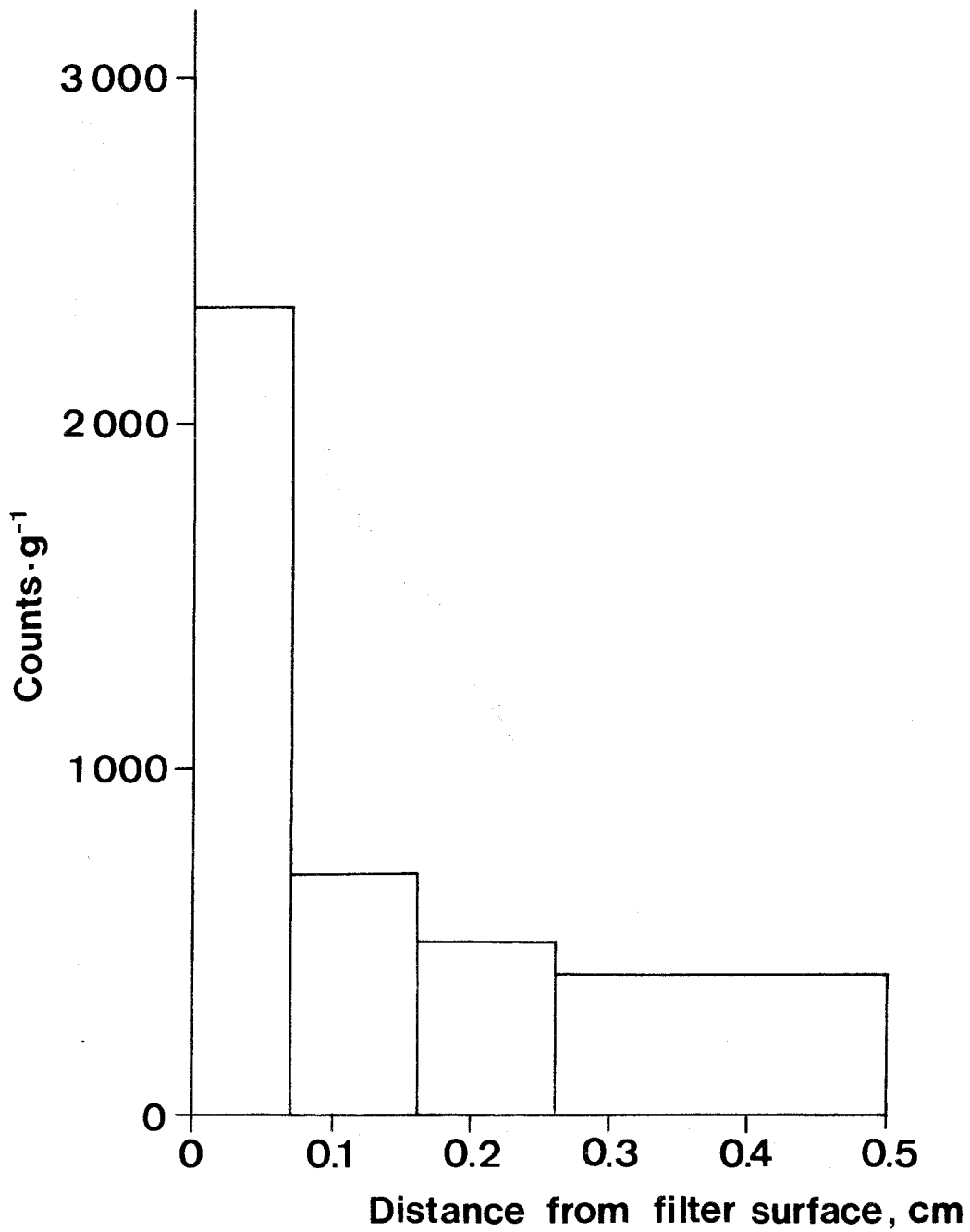


Fig. 10.  $I^-$ -concentration profile in 0.5 cm MX-80 disc after break-through test. Notice deviation from linear distribution.

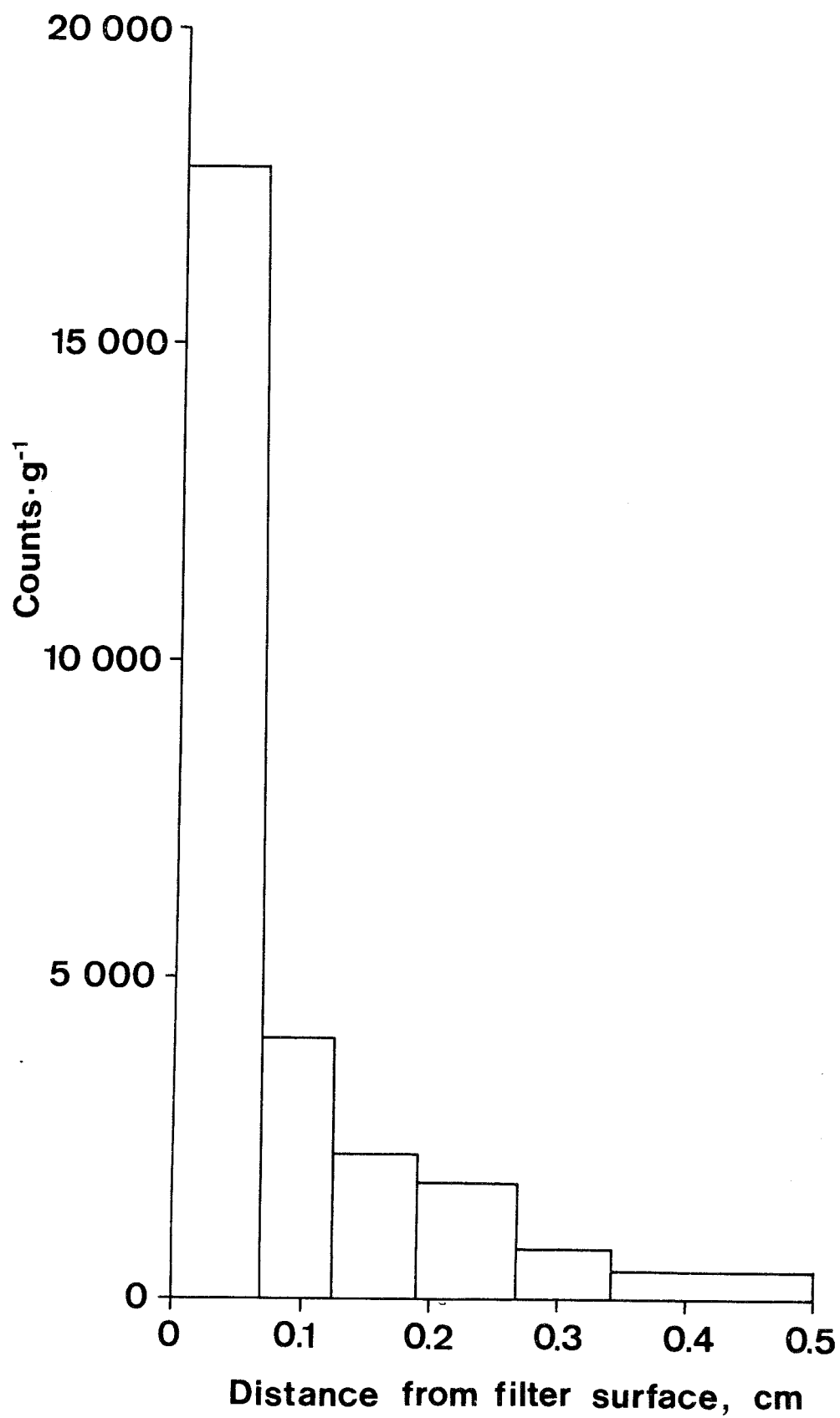


Fig. 11.  $\text{Cl}^-$ -concentration profile in 0.5 cm MX-80 disc break-through test.

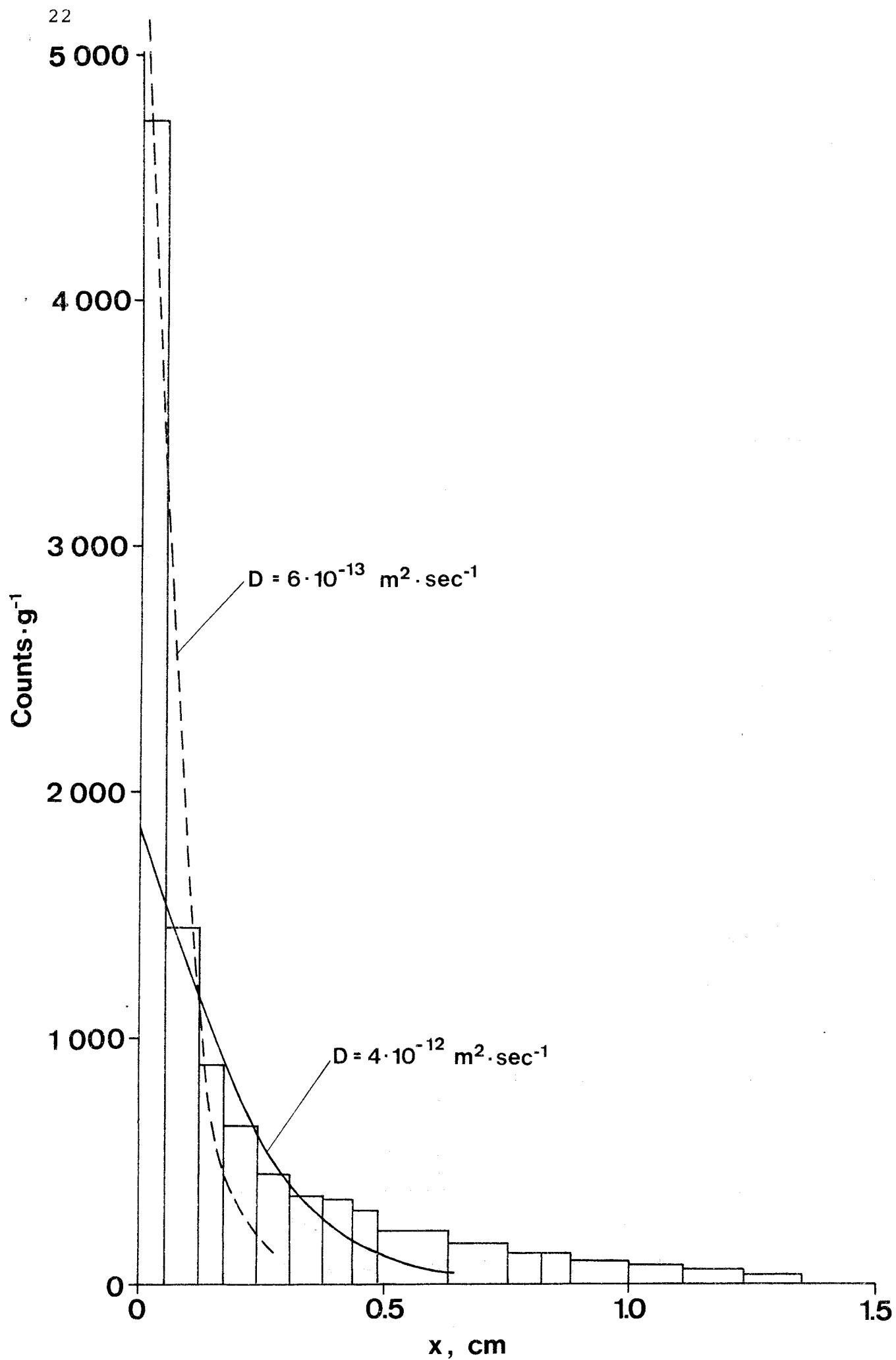


Fig. 12. Concentration profile of <sup>131</sup>I in MX-80 bentonite

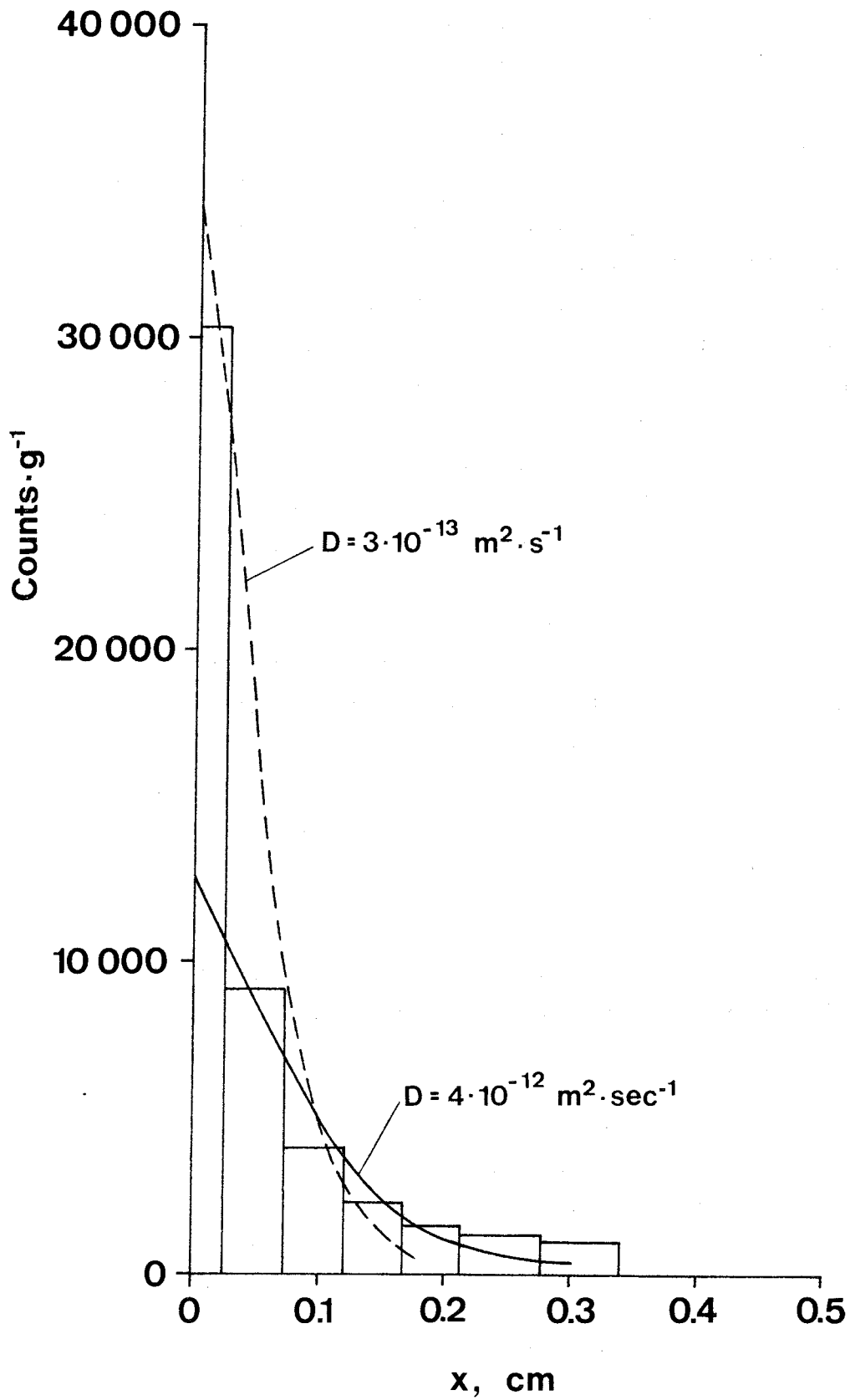


Fig. 13. Concentration profile of  $^{131}\text{I}$  in Erbslöh clay.

Concentration profiles of  $^{131}\text{I}$  diffusion into 20 mm long bentonite cylinders are shown in Figs. 12 and 13.

The graphs shown in Figs. 10-13 all show skewed radio-nuclide distributions with excessive concentrations at the interface between the clay and the tracer solution. This phenomenon is most probably related to the excess water at the bentonite/solution interface. Thus, as  $\text{I}^-$  and  $\text{Cl}^-$  are nonsorbing ions and therefore not enriched in the bentonite, a slight amount of excess water would result in the observed anomaly. The function  $c/C_0 = \text{erfc } x / (2 \sqrt{D_{\text{obs}} \cdot t})$  was first fitted to the experimental data taking into consideration the initial, very steep part of the recorded curves. This yielded very low values of the diffusion coefficients (broken lines in Figs. 12-13). The curve interpretation was then repeated but the activity of the surface layer was now omitted, which gave higher but more probable parameter values (full lines in the figures). The curve tails were given less weight because they are more uncertain due to greater corrections for background radiation. The latter diffusion coefficients are summarized in Table 3.

Table 3.  $D_{\text{obs}}$  for  $\text{I}^-$  and  $\text{Cl}^-$  diffusion as interpreted from break-through, and concentration profile tests.

Bentonite	Ion	Exp.method	$D_{\text{obs}} \text{ m}^2 \cdot \text{s}^{-1}$
MX-80	$\text{I}^-$	Break-through tests	$2.1 \cdot 10^{-13}$
Erbslöh	$\text{I}^-$	"-	$1.3 \cdot 10^{-13}$
MX-80	$\text{Cl}^-$	"-	$3.1 \cdot 10^{-13}$
MX-80	$\text{I}^-$	Concentration profile tests	$4 \cdot 10^{-12}$
Erbslöh	$\text{I}^-$	"-	$1 \cdot 10^{-12}$
MX-80	$\text{Cl}^-$	"-	$6 \cdot 10^{-12}$

It should be mentioned that the  $^{131}\text{I}$  and  $^{36}\text{Cl}$  concentrations in the bentonite were lower than expected. It is worth noticing also, that the  $D_{\text{obs}}$ -values for the investigated anions are two orders of magnitude lower than the values those reported for  $\text{CH}_4$  and  $\text{H}_2$  by NERETNIEKS (1978).

### DISCUSSION

A simple, straight-forward physical model would be that of pore diffusion which implies that the migration takes place in the pore water and that the ions are retarded by sorption processes. One-dimensional diffusion due to a concentration gradient is described by the following relationship:

$$\partial c / \partial t = D_w \partial^2 c / \partial x^2 \quad (3)$$

where  $c$  = concentration in the pore water ( $\text{mol}/\text{m}^3$ )  
 $t$  = time after onset of diffusion (s)  
 $D_w$  = diffusivity in water ( $\text{m}^2/\text{s}$ )  
 $x$  = distance from interface between tracer solution and clay sample (m)

In the case of sorption onto clay mineral surfaces we have, by definition:

$$q = K_d \cdot c \quad (4)$$

where  $q$  = concentration in solid ( $\text{mol}/\text{kg}$ )  
 $K_d$  = distribution coefficient ( $\text{m}^3/\text{kg}$ )

If  $K_d$  is taken as a constant, one-dimensional diffusion including sorption then takes the form:

$$\partial c / \partial t = D \partial^2 c / \partial x^2 - \rho_d \cdot \partial q / \partial t \quad (5)$$

where  $\rho_d = \frac{\text{mass of solid substance}}{\text{volume of solid and voids}}$  ( $\text{kg}/\text{m}^3$ )

Eqs. (4) and (5) yield:

$$\partial c / \partial t = D / (K_d \rho_d + 1) \partial^2 c / \partial x^2 \quad (6)$$

The latter D-parameter equals  $D_{\text{obs}}$  for the simple pore diffusion model so we can put:

$$D_{\text{obs}} = D_w / (1 + K_d \cdot \rho_d) \quad (7)$$

Since  $\rho_d$  is somewhat less than  $2 \text{ t/m}^3$  and  $K_d$  is known to be at least 50-100 this model suggests very low migration rates of  $\text{Sr}^{2+}$  and  $\text{Cs}^+$  compared to those of the non-sorbing ions  $\text{I}^-$  and  $\text{Cl}^-$ . This is in marked contrast to our experimental results which yield higher diffusivities for  $\text{Sr}^{2+}$  and  $\text{Cs}^+$  than for  $\text{I}^-$ ,  $\text{Cl}^-$ . This difference is in fact even more pronounced if the influence of the filter on cation migration is realized and if the observed low concentrations of the migrated anions are considered. The filter effect is obvious from the fact that the authors found  $K_d$  to be of the order of 40-100 in the diffusion experiments, while it was much higher in equilibrium tests (cf. Appendix 2). The effect is clearly manifested by the concentration anomaly discussed on page 16. While this indicates that the filter offers some diffusive resistance to the investigated cations, such resistance cannot have been the cause of the low concentration of  $\text{I}^-$  and  $\text{Cl}^-$  (cf. Appendix 2). Instead, it points to a considerable diffusive resistance of the clay/water system to the two anion species. This is amply shown by the fact that the break-through tests yielded very low values of the diffusion coefficient (cf. Table 3).

The authors' experiments indicate that ion diffusion through dense bentonite is governed by complex mechanisms which cannot be properly accommodated by pore diffusion models. Thus, it seems reasonable to believe that non-sorbing ions migrate in the pore water, while cations also move through smectite crystal lattices, preferably through interlamellar spacings and probably according to some "ion-exchange"-type

model. The very low diffusion rate of the investigated anions, as compared with the corresponding rate in bulk water, verifies that the diffusive resistance is very strong. Tortuosity in terms of passage irregularities contributes to this resistance but the major cause may well be the strong fixation and low mobility of the large majority of the water molecules in very dense bentonite, as concluded from permeability tests (PUSCH, 1981). Such tests have indicated that while water flow through clays of low density can be considered as the motion of a fluid with a definite and constant viscosity, it should rather be regarded as a shear-induced displacement of a "structured" medium in the case of dense bentonites. This is because the small interparticle distances imply that mineral-adsorbed water is largely involved in the flow process. In aged,

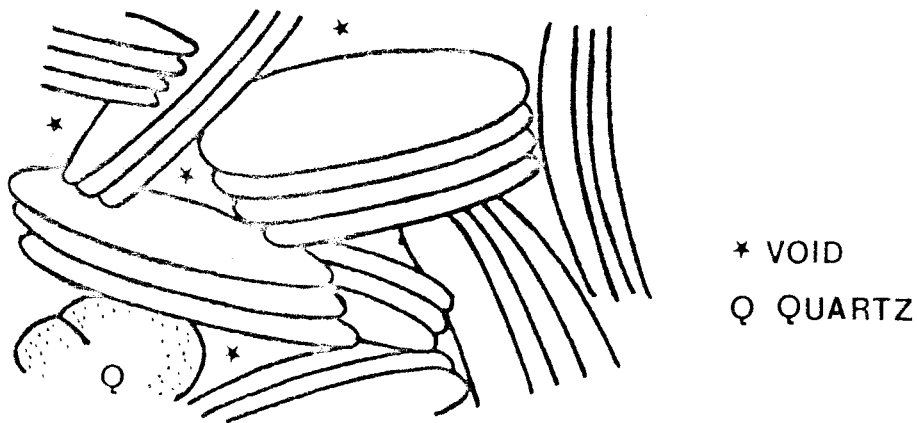


Fig. 14. Schematic picture of interparticle and interlamellar voids in dense bentonite.



homogeneous bentonite the largely constant interlamellar spacing is of the order of 5-15 Å for the bulk density interval 1.8-2.1 t/m<sup>3</sup>, which roughly corresponds to 2-4 water molecule layers<sup>1)</sup>. In practice, the varying particle geometry and orientation yield a variation in void size as well (Fig. 14) and it is reasonable to believe that only larger interparticle and intraparticle voids let water through. Such structural features can also be assumed to serve as main passages for anions and molecules (such as organic constituents) with no charge.

### CONCLUSIONS

The present study indicates different migration mechanisms for the diffusion of the investigated cations and anions, and it is shown, beyond doubt, that the diffusion rate of I<sup>-</sup> and Cl<sup>-</sup> is much lower than that of Sr<sup>2+</sup> and Cs<sup>+</sup> although the absolute values are somewhat uncertain. Determination of more reliable diffusion coefficients is necessary for a deepening of the understanding of the involved mechanisms as well as for practical application in the field of waste deposition. For this purpose, improved experimental technique is required so that the interface between different phases (solution/bentonite etc) is defined properly, and that filters are avoided. Such work is now in progress.

### REFERENCES

- JACOBSSON, A., 1974. Clay-water interaction. Diss. Dept. of Geology, University of Stockholm.
- NERETNIEKS, I., 1978. Diffusivitetmätningar av metan och väte i våt lera. KBS Teknisk Rapport 86.

---

<sup>1)</sup> Actually, the coordination of water molecules at silica surfaces does not imply a simple correlation between the spacing and the number of layers.

- PUSCH,R., 1980 a. Water uptake, migration, and swelling characteristics of unsaturated and saturated highly compacted bentonite. SKBF/KBS Teknisk Rapport 80-11.
- PUSCH,R., 1980 b. Permeability of highly compacted bentonite. SKBF/KBS Teknisk Rapport80-16.

Radionuclide sorption on bentonite

By Trygve Eriksen

According to the pore diffusion model for a porous solid the pore water diffusion is the dominating mass transfer mechanism. The diffusivity of a radionuclide in bentonite should therefore be influenced by parameters such as porosity and tortuosity as well as sorption, ion exchange and other reactions between the radionuclide and the bentonite. If these processes are fast and reversible local equilibrium can be assumed to exist between the free and immobilized components of the diffusing substance. This equilibrium can be described by the equation

$$q = K_d \cdot c \quad (1)$$

where  $q$  = concentration in solid ( $\text{mol} \cdot \text{g}^{-1}$ )

$c$  = concentration in solution ( $\text{mol} \cdot \text{cm}^{-3}$ )

and  $K_d$  = distribution coefficient ( $\text{cm}^3 \cdot \text{g}^{-1}$ )

and the diffusion by (Crank)

$$\partial c / \partial t = D \cdot \partial^2 c / \partial x^2 - \rho \partial q / \partial t \quad (2)$$

where  $\rho$  = density of solid ( $\text{g} \cdot \text{cm}^{-3}$ )

Combining equation 1 and 2 we obtain

$$\partial c / \partial t = (D / (1 + K_d \cdot \rho)) \partial^2 c / \partial x^2 \quad (3)$$

i.e. according to the pore diffusion model the diffusivity of a sorbing radionuclide will be decreased by a factor  $(1 + K_d \rho)$  as compared to a nonsorbing radionuclide.

The distribution coefficients for radionuclides varying by several orders of magnitude are therefore of great importance in evaluation of radionuclide migration data. As the diffusion experiments were carried out with com-

pacted bentonite (density  $2.1 \pm 0.1 \text{ g} \cdot \text{cm}^{-3}$ ) it was of interest to see if the higher density (and thereby possible changes in liquid/solid contact area) have any effect on the distribution coefficients.

### Experimental

The experiments were carried out with the two bentonites used in the diffusion experiments i.e. American Colloid Co type Mx-80 (Na-bentonite) and Bavarian Erbslöh Ca-bentonite. In all experiments Allard-water was used.  $^{85}\text{Sr}$  and  $^{131}\text{Cs}$  were used as tracers.

Two series of experiments were carried out:

#### Series 1

The radionuclides were obtained in aqueous stock solutions as follows:

$^{85}\text{Sr}$  in 0.5 HCl and  $^{134}\text{Cs}$  as CsCl.

Tracer solutions were prepared by dilution of small aliquots of stock solutions by Allard water.

Air dry bentonite was compacted to the density required in the LuH swelling oedometer (figure 4 report) and water contacted for 15 days.

The dimensions of the bentonite sample was area  $19.56 \text{ cm}^2$ , thickness 0.5 cm. The water was then replaced by  $24 \text{ cm}^3$  tracer solution which was connected to both the upper and lower filter-stone. Continuous circulation was applied to yield uniform radionuclide concentration.

Measured volumes (0.1 ml) of the radionuclide were analyzed by liquid scintillation counting.

After 30 days equilibrium was judged to prevail. The oedometers were then opened and the bentonite sliced into 0.52 mm thick samples. The samples were weighted and the radionuclide concentration measured by counting in 3" x 3" NaI well type detector.

$K_d$ -values were calculated using the following expression

$$K_d = \frac{V}{W} \cdot \frac{C_o - C_{eq}}{C_{eq}}$$

where  $V$  = volume of tracer solution

$W$  = mass of bentonite

$C_o$  = net count rate of feed solution

$C_{eq}$  = net count of solution at equilibrium

### Series 2

25, 50 and 100 mg bentonite samples were batch contacted with 25 ml tracer solution. The solutions were agitated for 24 h at room temperature and after contacting the solutions were either pressure filtered through at 0.8  $\mu$ m Millipore filter or centrifugated. Measured volumes of the liquid phase as well as the bentonite were analyzed by radiation counting.

Counting was done with a 3" x 3" sodium iodide well type scintillation detector. Values for  $K_d$  were calculated using the following expression

$$K_d = \frac{V}{W} \cdot C_s / C_\ell$$

Where  $V$  = volume of tracer solution added to the batch sample ( $\text{cm}^3$ )

$W$  = mass of solid added to the batch sample (g)

$C_s$  = net count rate per unit weight solid

$C_\ell$  = net count rate per unit volume of tracer solution after contracting

## Results

The temporal change in radionuclide concentration expressed as the fraction  $C/C_0$  are depicted in figures 1 and 2. The rate of decrease in radionuclide concentration was governed by the diffusive transport through the filter-stones and the compacted bentonite. Near constant radionuclide concentration in solution was obtained after  $\sim 10$  days with the exception of  $^{134}\text{Cs}^+$  in Erbslöh bentonite. Here a sharp decrease in  $^{134}\text{Cs}$  concentration during the first 2-3 days was followed by a continuous slower decrease for at least 30 days.

The  $^{134}\text{Cs}$  distributions within the bentonites are depicted in figures 3 and 4. As seen there is some variation in  $^{134}\text{Cs}$  concentration within the bentonite.

The calculated  $K_d$ -values from series 1 and 2 are summarized in table 1.

Table 1

Bentonite	$K_d$	$K_d$	Exp. cond.
	$\text{cm}^3 \cdot \text{g}^{-1}$	$\text{cm}^3 \cdot \text{g}^{-1}$	
	$^{85}\text{Sr}$	$^{134}\text{Cs}$	
MX-80	604	645	Compacted
	645, 1315	1374, 1462, <sup>a)</sup> 224	batch
Erbslöh	421	1407 (4 days)	Compacted
		>8500	
	552, 549	<sup>a)</sup> 1050, 2760,	batch
		<sup>a)</sup> 2290	
		(>10 <sup>4</sup> )	

a) filtered

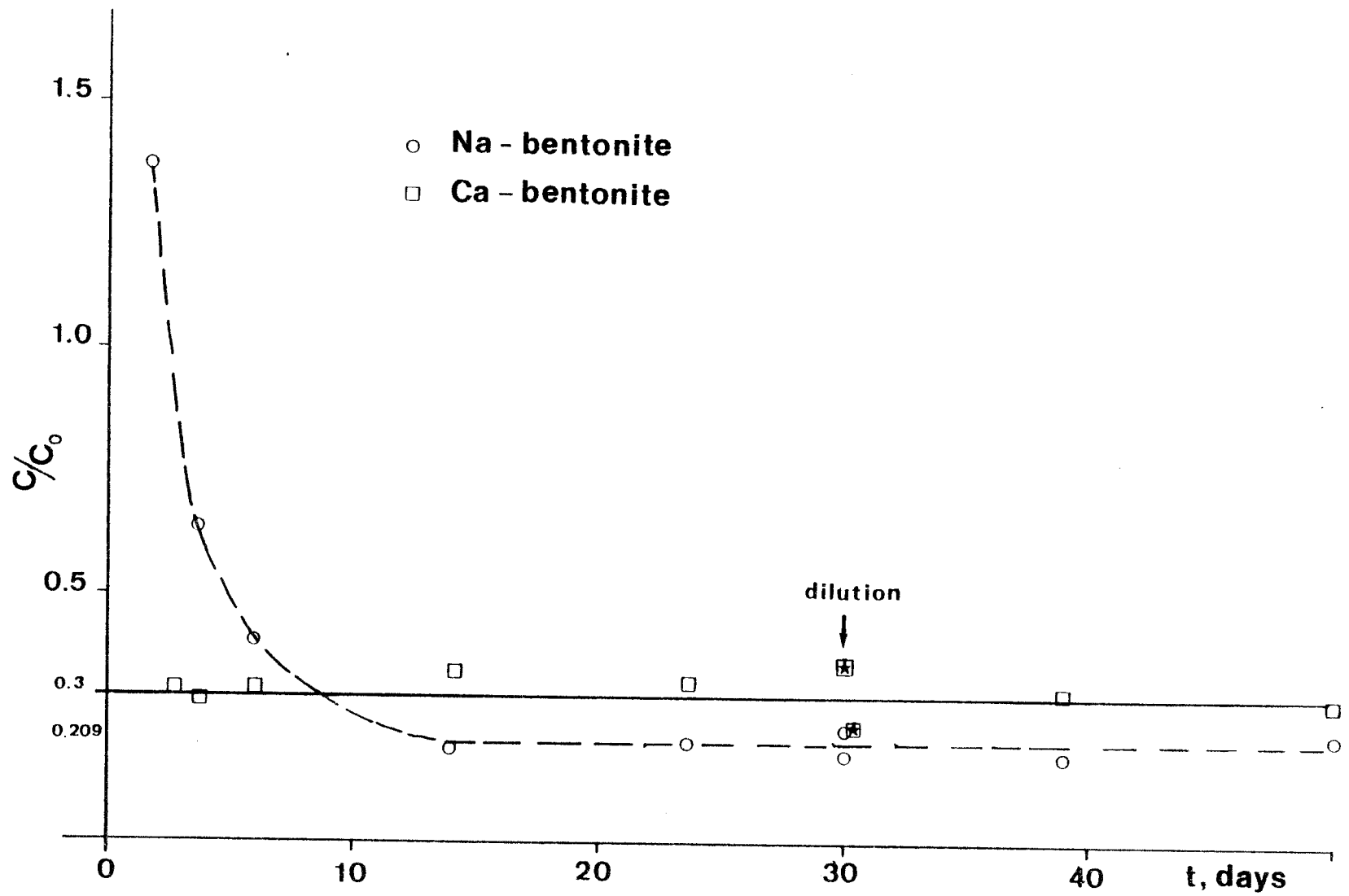


Fig. 1 Relative  $^{85}\text{Sr}$  concentration in solution vs time of contact with compacted bentonites.  
 $W = 20.62 \text{ g}, V = 24 \text{ cm}^3$

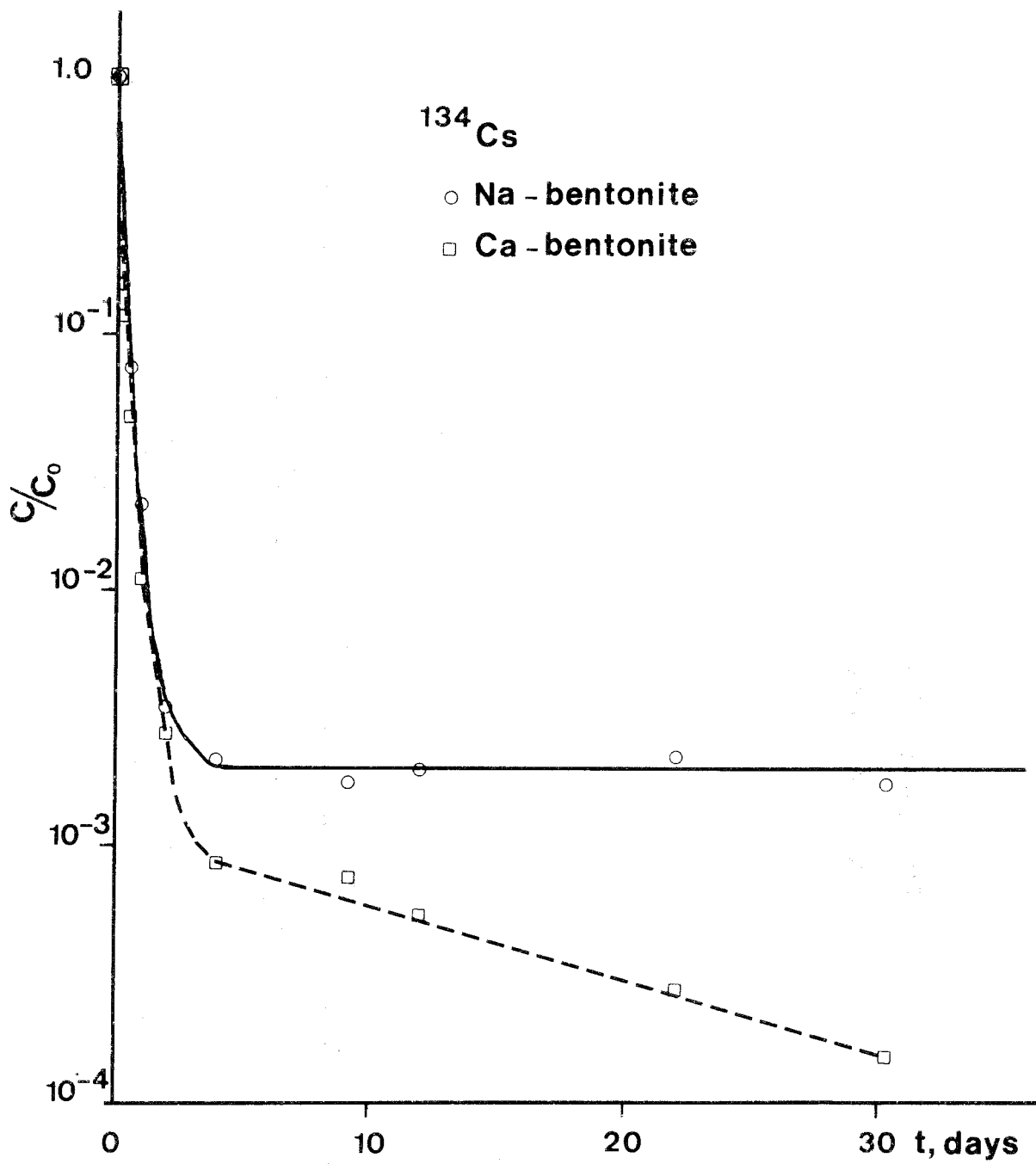


Fig. 2. Relative concentration of  $^{134}\text{Cs}$  in solution vs time of contact with bentonite  $W = 20.62 \text{ g}$ ;  $V = 24 \text{ cm}^3$ .



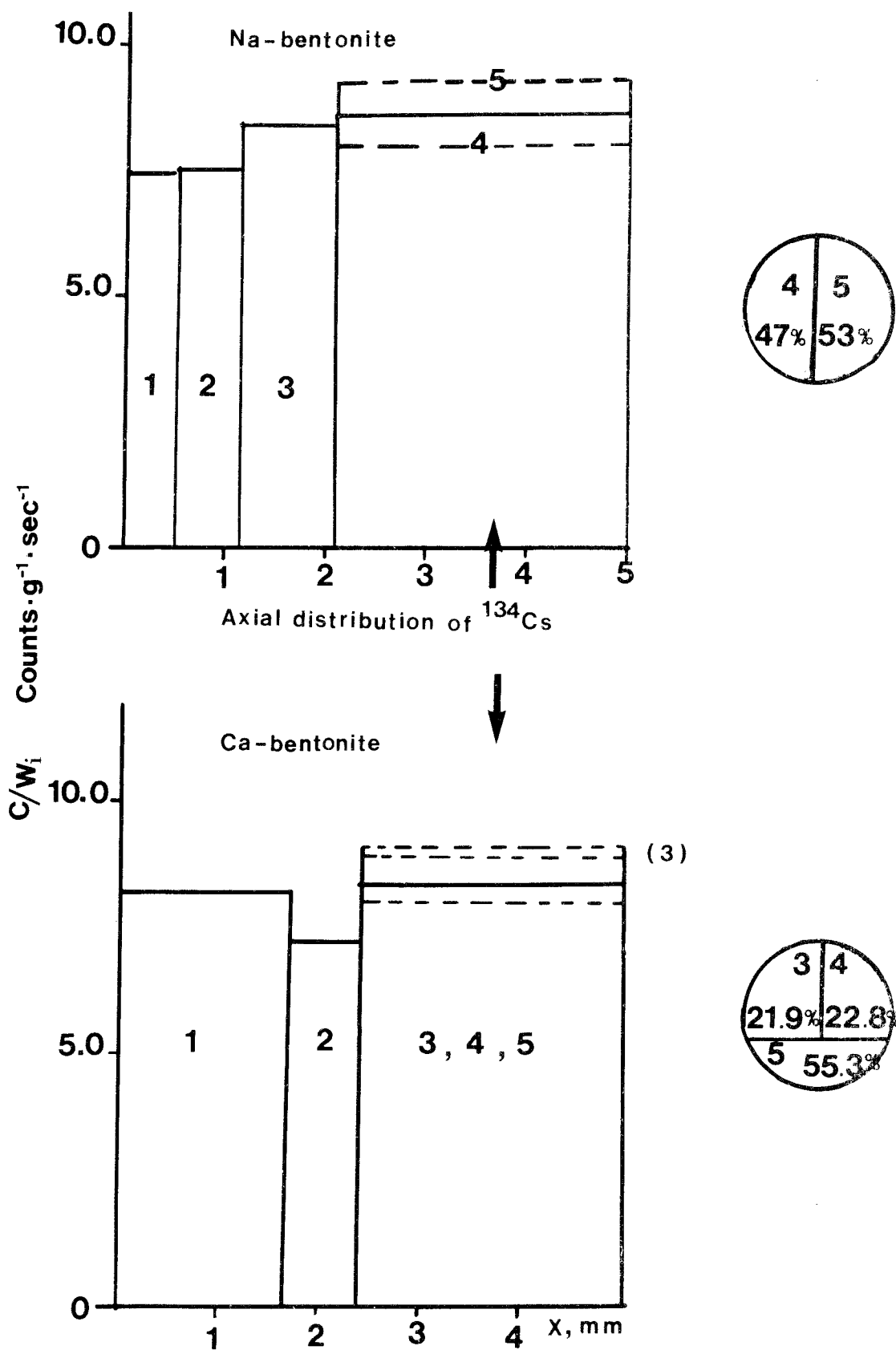


Fig. 3-4. <sup>134</sup>Cs distributions within the actual bentonites showing some variation in <sup>134</sup>Cs concentration.

### Discussion

The  $K_d$ -values for  $^{85}\text{Sr}$  were found to be approximately equal for the two different bentonites and independent of the experimental technique used. The results obtained for  $^{134}\text{Cs}$  show a greater scatter but give an average slightly higher values for the batch-equilibration technique. Two interesting observations can be made from figure 2 and table 1. In one of the batch experiments the  $^{134}\text{Cs}$  concentration in the liquid phase was very low after equilibration and no exact calculation of  $K_d$  could be made. A lower limit of  $10^4 \text{ cm}^3 \cdot \text{g}^{-1}$  is given. This effect is possibly due to non representative composition of the small amount of bentonite used or to impurities in the bentonite.

From figure 1 it is seen that equilibrium was not obtained in Erbslöh bentonite 30 days of contact with radionuclide solution. The slower process may possibly be due to fixation of  $^{134}\text{Cs}$  in the bentonite. The  $K_d$ -values obtained are generally as could be expected 2-3 times higher for  $^{134}\text{Cs}$  than for  $^{85}\text{Sr}$ .

### Reference

J CRANK: The Mathematics of Diffusion, Oxford University Press, Oxford 1956.

Diffusion through filter-stones

By Trygve Eriksen

In the diffusion experiments with LuH oedometers the compacted bentonite was confined between two filter-stones through which the radionuclides had to diffuse before reaching the bentonite. In order to assess the effect of the diffusive resistance of the filter-stones a study of the diffusion of  $\text{Cs}^+$ ,  $\text{Sr}^{2+}$  and  $\text{I}^-$  was carried out.

Experimental

The filter-stones Porosint stainless steel P/2.5 used were of two types, a simple filter (diameter 49.7 mm, thickness 3.75 mm) and composite filter (diameter 49.7 mm, thickness 7.4 mm). The filters were mounted in the diffusion cells (figure 1) and the cells were then washed with Allard water. The cell compartments were thereafter filled with Allard water and small aliquots of radionuclide solutions (60.5 ml) added to one compartment in each diffusion cell. The solutions were stirred with magnetic stirrers to ensure homogeneous concentration in each compartment and small sample volumes were drawn from each compartment at different periods to monitor the changes in radionuclide concentration.  $^{85}\text{Sr}$ ,  $^{134}\text{Cs}$  and  $^{131}\text{I}$  were used as tracer nuclides and their concentrations determined by  $\gamma$ -counting in a 3"x3" NaI well type scintillation detector. All experiments were carried out at ambient temperature.

The diffusivities were calculated from the equation

$$V_2 \frac{dc_2}{dt} = D \cdot A \cdot \frac{(C_1 - C_2)}{x}$$

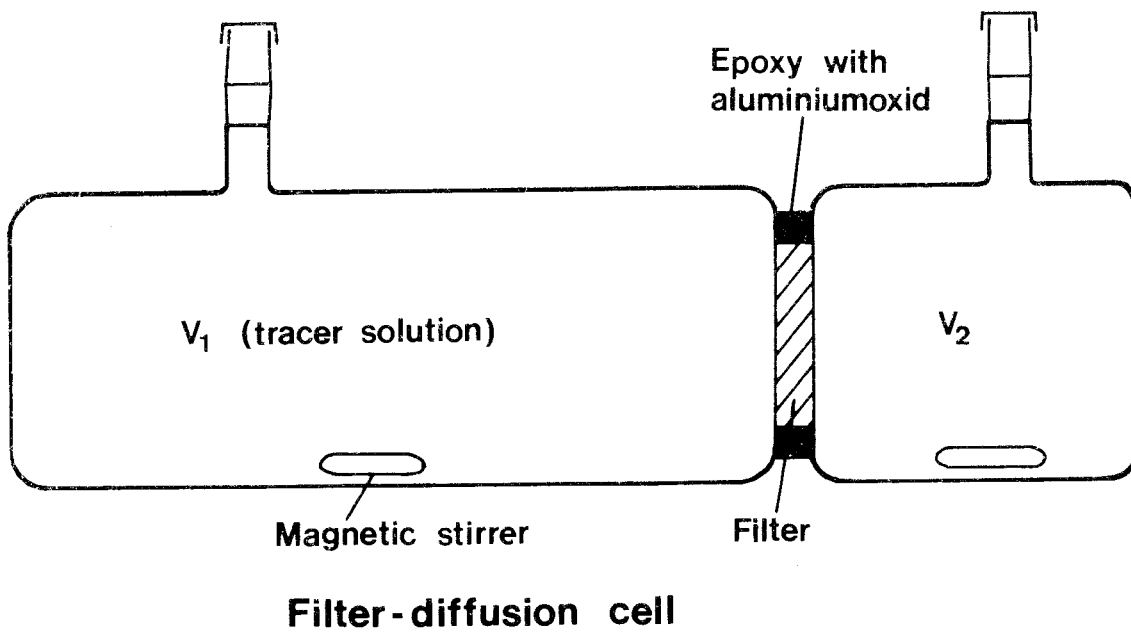


Fig. 1.

where  $D$  = diffusivity  $\text{cm}^2 \cdot \text{sec}^{-1}$

$C_2$  = radionuclide concentration in low activity compartment ( $\text{counts} \cdot \text{cm}^{-3} \cdot \text{sec}^{-1}$ )

$C_1$  = radionuclide concentration in high activity compartment

$A$  = contact area of filterstone ( $\text{cm}^2$ )

$x$  = thickness of filterstone (cm)

$t$  = time ( $\text{sec}^{-1}$ )

### Results

Typical plots of the changes in radionuclide concentration on the low activity side of a filterstone vs time after onset of diffusion are depicted in figure 2. Computed diffusivities for  $\text{Sr}^{2+}$ ,  $\text{Cs}^+$  and  $\text{I}^-$  are given in table 1.

Table 1.

Filter	Ion	<sup>1)</sup> $D \cdot 10^6 \text{ cm}^2 \cdot \text{sec}^{-1}$
Single	$\text{Sr}^{+2}$	0.53
	$\text{Cs}^+$	1.5
	$\text{I}^-$	1.8
Composite	$\text{Sr}^{2+}$	0.51
	$\text{Cs}^+$	1.37
	$\text{I}^-$	1.20

<sup>1)</sup> based on geometric surface

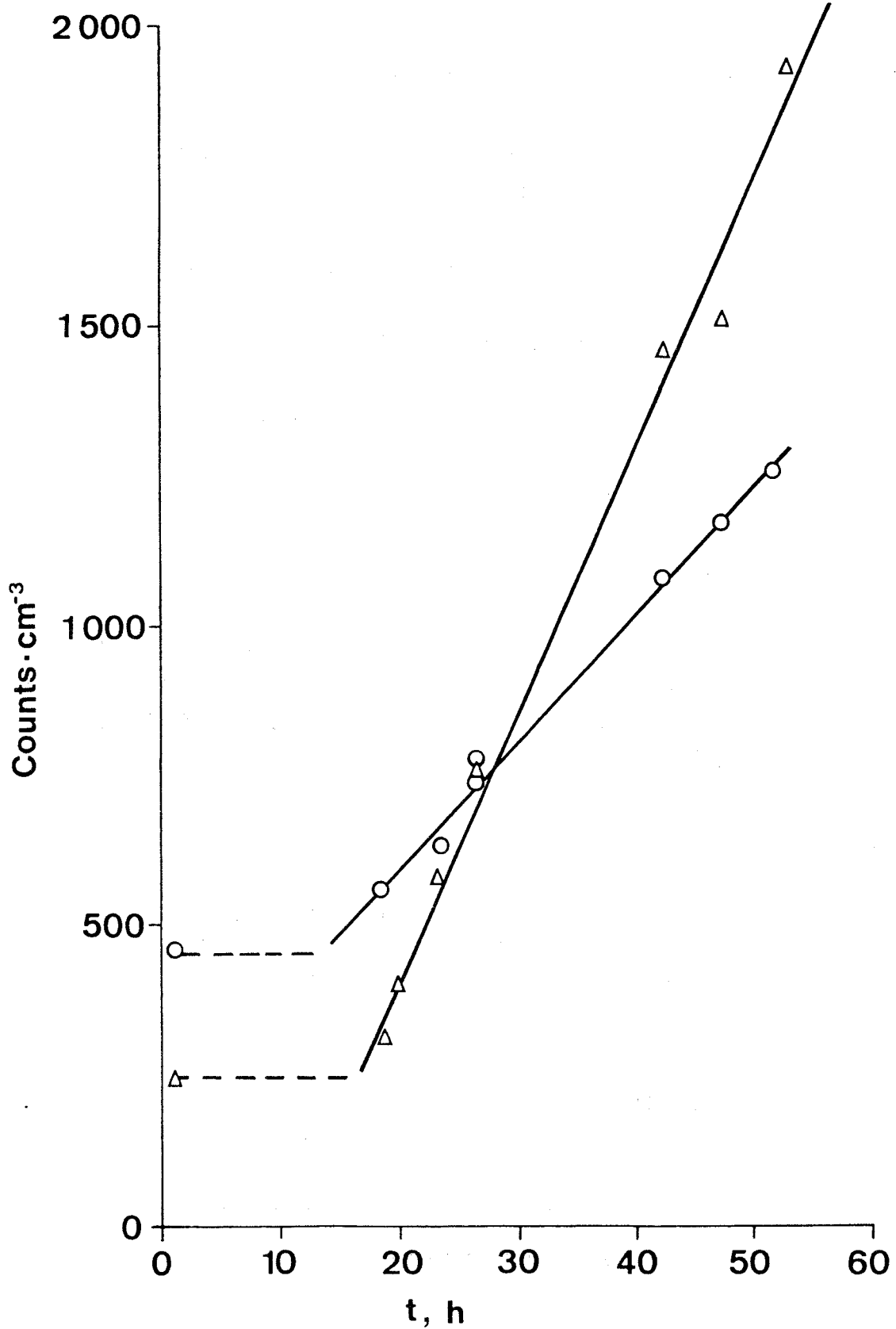


Fig. 2. Diagram of "break-through" of  $^{85}\text{Sr}^{2+}$  and  $^{134}\text{Cs}^+$

### Discussion

The rather high diffusivities clearly show that the diffusion resistance in the filter-stones has not been a limiting factor in the  $\text{Cl}^-$  and  $\text{I}^-$  diffusion experiments. In the case of  $\text{Sr}^{2+}$  and  $\text{Cs}^+$ , however, the diffusion resistance in the filter-stones has clearly been a limiting factor. The effect of this is probably that the concentration profiles in the bentonites are somewhat stretched in the x-direction and the computed diffusivities therefore somewhat too high.

## FÖRTECKNING ÖVER KBS TEKNISKA RAPPORTER

### 1977-78

TR 121 KBS Technical Reports 1 - 120.  
Summaries. Stockholm, May 1979.

### 1979

TR 79-28 The KBS Annual Report 1979.  
KBS Technical Reports 79-01--79-27.  
Summaries. Stockholm, March 1980.

### 1980

TR 80-26 The KBS Annual Report 1980.  
KBS Technical Reports 80-01--80-25.  
Summaries. Stockholm, March 1981.

### 1981

TR 81-01 A note on dispersion mechanisms in the ground  
Ivars Neretnieks  
Royal Institute of Technology, March 1981

TR 81-02 Radiologisk exponering från strandsediment  
innehållande torium-229  
Karl Anders Edvardsson  
Sverker Evans  
Studsvik Energiteknik AB, 1981-01-27

TR 81-03 Analysis of the importance for the doses of  
varying parameters in the biopath-program  
Ulla Bergström  
Studsvik Energiteknik AB, 1981-03-06

TR 81-04 Uranium and radium in Finnsjön - an experimental  
approach for calculation of transfer factors  
Sverker Evans  
Ronny Bergman  
Studsvik Energiteknik AB, 1981-05-07



- TR 81-05 Canister materials proposed for final disposal  
of high level nuclear waste - a review with  
respect to corrosion resistance  
Einar Mattsson  
Swedish Corrosion Institute, Stockholm, June 1981
- TR 81-06 Ion diffusion through highly compacted bentonite  
Trygve Eriksen  
Department of Nuclear Chemistry  
Royal Institute of Technology, Stockholm  
Arvid Jacobsson  
Roland Pusch  
Division Soil Mechanics, University of Luleå  
1981-04-29